Dynamic Visualization of Thrombopoiesis Within Bone Marrow

Science

AAAS

counteract the activity of miRNAs in cancer development and progression.

References and Notes

1. V. Ambros, *Nature* **431**, 350 (2004).
2. N. Bushati, S. M. Cohen, *Annu. Rev. Cell Dev. Biol.* published online 21 May 2007, 10.1146/annurev.cellbio.23.090506.123406, in press.
3. W. P. Kloosterman, R. H. Plasterk, *Dev. Cell* **11**, 441 (2006).
4. C. Z. Chen, L. Li, H. F. Lodish, D. P. Bartel, *Science* **303**, 83 (2004).
5. T. Du, P. D. Zamore, *Development* **132**, 4645 (2005).
6. L. He, G. J. Hannon, *Nat. Rev. Genet.* **5**, 522 (2004).
7. G. Meister, T. Tuschl, *Nature* **431**, 343 (2004).
8. R. S. Pillai, S. N. Bhattacharyya, W. Filipowicz, *Trends Cell Biol.* **17**, 118 (2007).
9. R. J. Jackson, N. Standart, *Sci. STKE* **2007**, re1 (2007).
10. R. S. Pillai *et al.*, *Science* **309**, 1573 (2005).
11. D. T. Humphreys, B. J. Westman, D. I. Martin, T. Preiss, *Proc. Natl. Acad. Sci. U.S.A.* **102**, 16961 (2005).
12. C. P. Petersen, M. E. Bordeleau, J. Pelletier, P. A. Sharp, *Mol. Cell* **21**, 533 (2006).
13. S. Bagga *et al.*, *Cell* **122**, 553 (2005).
14. L. Wu, J. Fan, J. G. Belasco, *Proc. Natl. Acad. Sci. U.S.A.* **103**, 4034 (2006).
15. S. Nottrott, M. J. Simard, J. D. Richter, *Nat. Struct. Mol. Biol.* **13**, 1108 (2006).
16. I. Behm-Ansmant *et al.*, *Genes Dev.* **20**, 1885 (2006).
17. P. H. Olsen, V. Ambros, *Dev. Biol.* **216**, 671 (1999).
18. Y. V. Svitkin, N. Sonenberg, *Methods Mol. Biol.* **257**, 155 (2004).
19. A. Kahvejian, Y. V. Svitkin, R. Sukarieh, M. N. M'Boutchou, N. Sonenberg, *Genes Dev.* **19**, 104 (2005).
20. Materials and methods are available as supporting material on *Science* Online.
21. C. K. Raymond, B. S. Roberts, P. Garrett-Engele, L. P. Lim, J. M. Johnson, *RNA* **11**, 1737 (2005).
22. T. V. Pestova, C. U. Hellen, I. N. Shatsky, *Mol. Cell. Biol.* **16**, 6859 (1996).
23. M. Kiriakidou *et al.*, *Cell* **129**, 1141 (2007).
24. R. Thermann, M. W. Hentze, *Nature* **447**, 875 (2007).
25. T. P. Chendrimada *et al.*, *Nature* **447**, 823 (2007).
26. P. A. Maroney, Y. Yu, J. Fisher, T. W. Nilsen, *Nat. Struct. Mol. Biol.* **13**, 1102 (2006).
27. B. Wang, T. M. Love, M. E. Call, J. G. Doench, C. D. Novina, *Mol. Cell* **22**, 553 (2006).
28. A. Esquela-Kerscher, F. J. Slack, *Nat. Rev. Cancer* **6**, 259 (2006).
29. Y. Mamane *et al.*, *Oncogene* **23**, 3172 (2004).
30. We thank M. Costa-Mattioli, A. Rosenfeld, and D. Arvanitis for comments. Supported by Human Frontiers Science Foundation (N.S.), Howard Hughes Medical Institute (E.D.), NIH (W.C.M.). Postdoctoral support by Fonds de Recherche en Santé du Québec (FRSQ) to G.M., Natural Sciences and Engineering Research Council and Richard H. Tomlinson (M.R.F.), Fonds National Suisse (L.H.), Japanese Society for the Promotion of Science (T.M.), Canadian Institute of Health Research and FRSQ awards (T.F.D.). Friedrich Miescher Institute is supported by the Novartis Research Foundation.

Dynamic Visualization of Thrombopoiesis Within Bone Marrow

Tobias Junt,[1] Harald Schulze,[2]* Zhao Chen,[2] Steffen Massberg,[1] Tobias Goerge,[1] Andreas Krueger,[2]† Denisa D. Wagner,[1] Thomas Graf,[4] Joseph E. Italiano Jr.,[3] Ramesh A. Shivdasani,[2]‡ Ulrich H. von Andrian[1]‡

Platelets are generated from megakaryocytes (MKs) in mammalian bone marrow (BM) by mechanisms that remain poorly understood. Here we describe the use of multiphoton intravital microscopy in intact BM to visualize platelet generation in mice. MKs were observed as sessile cells that extended dynamic proplatelet-like protrusions into microvessels. These intravascular extensions appeared to be sheared from their transendothelial stems by flowing blood, resulting in the appearance of proplatelets in peripheral blood. In vitro, proplatelet production from differentiating MKs was enhanced by fluid shear. These results confirm the concept of proplatelet formation in vivo and are consistent with the possibility that blood flow–induced hydrodynamic shear stress is a biophysical determinant of thrombopoiesis.

Blood platelets are required to maintain hemostasis in mammals. The relative paucity of MKs in normal BM contrasts with the relative abundance of platelets in peripheral blood and implies that platelet assembly and release are highly efficient, dynamic processes. The prevalent model for thrombopoiesis, the proplatelet or flow model (*1, 2*), receives support mostly from MK differentiation cultures (*3–5*), which deprive MKs of cellular contacts and signals found in intact BM (*6, 7*). The flow model proposes that MKs extend plump pseudopodia that give rise to long (>100-μm) branched proplatelet processes that appear "beaded" by virtue of intermediate swellings (*3, 4, 8*). It is unclear whether proplatelets detach from MKs in bulk and fragment further into platelets (*4*) or whether barbell-shaped platelet pairs detach exclusively from proplatelet ends (*8*), but eventually the MK cytoplasm is exhausted as a result of fragment release. Previous in situ imaging approaches, such as electron microscopy, helped define the morphology and environment of MKs in the BM (*1, 2, 9*), but they provided only static snapshots that leave room for alternative mechanistic concepts of thrombopoiesis. For example, the platelet territory model proposes that vesicles from internal MK demarcation membranes are released as mature platelets (*10–12*). Another conundrum pertains to how newly formed platelets traverse BM vessel walls and escape activation by subendothelial prothrombotic factors.

To observe thrombopoiesis in vivo, we studied mouse skull BM by multiphoton intravital microscopy (MP-IVM) (*13, 14*). To identify MKs and their progeny, we used $CD41\text{-}EYFP^{ki/+}$ mice in which enhanced yellow fluorescent protein (EYFP) was expressed as a targeted transgene from the endogenous gene locus for *CD41*, an MK- and platelet-specific integrin (*15*). We used heterozygous $CD41\text{-}EYFP^{ki/+}$ mice and confirmed that EYFP$^+$ MKs in BM of these animals generate fully functional platelets at normal frequency (fig. S1).

MKs showed considerable morphological diversity; they occurred mostly as isolated cells but occasionally in clusters, and they were always found in close contact with BM sinusoids (Fig. 1, A and B, and movie S1). MKs were largely sessile, exhibiting minimal migratory tracks or three-dimensional (3D) instantaneous velocities as compared with other BM-resident cell types (Fig. 1C). To facilitate imaging of normally rare MKs, we pretreated some mice with thrombopoietin (TPO), which increased MK numbers but did not alter their perivascular localization (fig. S2 and movie S2). Another physiologic activity of TPO is the differentiation of immature MKs, which are small and compact, toward larger mature cells that assemble and release platelets (*16*). Indeed, 3D reconstructions of intravital recordings (Fig. 1, D and E) revealed that TPO treatment increased maximal MK diameters (Fig. 1F) and volumes (Fig. 1G) and caused more irregular MK shapes (Fig. 1H).

Many MKs exhibited fragmented protrusions (Fig. 1, I and J, and movie S3), whereas others were surrounded by scattered EYFP$^+$ particles (Fig. 1A and movie S4), which may represent proplatelets that remained connected to the MK cell body. However, particle connections were mostly inferred based on near-linear alignment and close proximity of particles to large MK bodies (Fig. 1J), because insuffi-

[1]Immune Disease Institute and Department of Pathology, Harvard Medical School, Boston, MA 02115, USA. [2]Dana-Farber Cancer Institute, Boston, MA 02115, USA. [3]Hematology Division, Brigham and Women's Hospital, Boston, MA 02115, USA. [4]Centre de Regulacio Genomica, Parc de Recesca Biomedica de Barcelona, 08003 Barcelona, Spain.

*Present address: Klinik für Allgemeine Pädiatrie, Charite, Labor für Pädiatrische Molekularbiologie, 10117 Berlin, Germany.
†Present address: Institute of Immunology, Hannover Medical School, 30625 Hannover, Germany.
‡To whom correspondence should be addressed. E-mail: uva@hms.harvard.edu (U.H.v.A.); ramesh_shivdasani@dfci.harvard.edu (R.A.S.)

cient signal intensity limited direct visualization. The farnesylated EYFP reporter protein in $CD41\text{-}EYFP^{ki/+}$ MK localizes to external and internal membranes (15, 17); intermediate and distal proplatelet swellings contain numerous internal membranes and thus generate a robust fluorescent signal, whereas proplatelet shafts contain little membrane (18) and tend to fall below the detection limit. Nevertheless, we captured the formation of MK fragments on 1- to 2-μm-thick, branching filaments budding from one MK pole (fig. S3A and movie S5), reminiscent of proplatelet formation in vitro (8). Consistent with TPO-induced MK maturation, interstitial MK fragments tended to be smaller in TPO-treated mice (Fig. 1K). However, almost all MK fragments were 10 to 100 times as large as circulating platelets (Fig. 1K), implying that few mature platelets get released within the BM interstitium. Most EYFP⁺ fragments in the BM were immotile, but some moved with a median 3D instantaneous velocity of 3.9 μm/min (fig. S3, B and C, and movie S6). Because proplatelet elongation from cultured MKs occurs at ~0.85 μm/min (19), these observations suggest that the BM microenvironment enhances the motility of MK extensions.

Consistent with ultrastructural observations (1, 2, 20), MKs extended cellular processes into BM microvessels in TPO-treated and untreated mice (Fig. 2A, movie S7, and fig. S2). These intravascular EYFP⁺ extensions had a mean volume of 3295 μm³ (Fig. 2B), corresponding to ~6% of the average MK volume or 824 times the mean volume of mature murine platelets (4 μm³). These fragments may represent multiple intertwined or single immature proplatelets. MP-IVM recordings also captured MKs extending plump perivascular pseudopodia, reportedly the first step of platelet release in vitro (8, 18), over the span of <15 min (Fig. 2C and movie S8). On one occasion, an unusually large EYFP⁺ MK fragment entered a BM vessel, and intravascular fluorescein isothiocyanate (FITC)–dextran tracer accumulated upstream, indicating transient vascular occlusion (Fig. 2D and movie S9). Such observations imply that BM sinusoidal diameter imposes size constraints on released MK fragments and that transsinusoidal migration of whole MKs (21) is probably rare. Smaller, spherical MK fragments typically protruded through the sinusoidal wall (Fig. 2E), moved in the direction of blood flow, and were eventually released into the lumen, either slowly along the endothelium (Fig. 2E and movie S10) or briskly (movie S11).

These observations collectively reveal that MKs routinely release heterogeneous particles, with properties resembling immature proplatelets, into BM microvessels. Shedding events in TPO-treated mice were recorded about once every 7 hours per field of view. Even these seemingly infrequent events likely contribute substantially toward physiological platelet outputs. Assuming that the platelet lifespan is 5 to 6 days and that TPO treatment doubled the normal

platelet number in mice [~2.2 × 10⁹ to ~4.4 × 10⁹ platelets (22)], we calculate the steady-state platelet production in TPO-treated animals as 0.8 × 10⁹ platelets per day. Mouse BM and spleen contain a total of ~180,000 MKs (14), whose number is also doubled after TPO treatment (22). If each MK releases one fragment every 7 hours, the total intravascular discharge amounts to 1.2 × 10⁶ fragments per 24 hours, with a combined mean volume (Fig. 2B) corresponding to ~1 × 10⁹ platelets. Thus, even if we consider that proplatelet cytoplasmic mass may not completely convert into mature platelets as it diminishes during further fragmentation (8, 18),

these calculations suggest that intravascular proplatelet shedding by juxtasinusoidal MKs may account for the bulk of thrombopoiesis. However, it should be cautioned that we cannot exclude additional thrombopoieitic events that may occur below the limit of MP-IVM resolution or in regions that are inaccessible to intravital imaging.

To assess how intravascular shedding of MK fragments relates to the presumptive MK maturation sequence, we first classified nonshedding MKs in TPO-treated mice into two groups ("small" and "large") according to how their maximal diameter related to the mean diameter calculated in Fig. 1F. Based on 3D reconstruc-
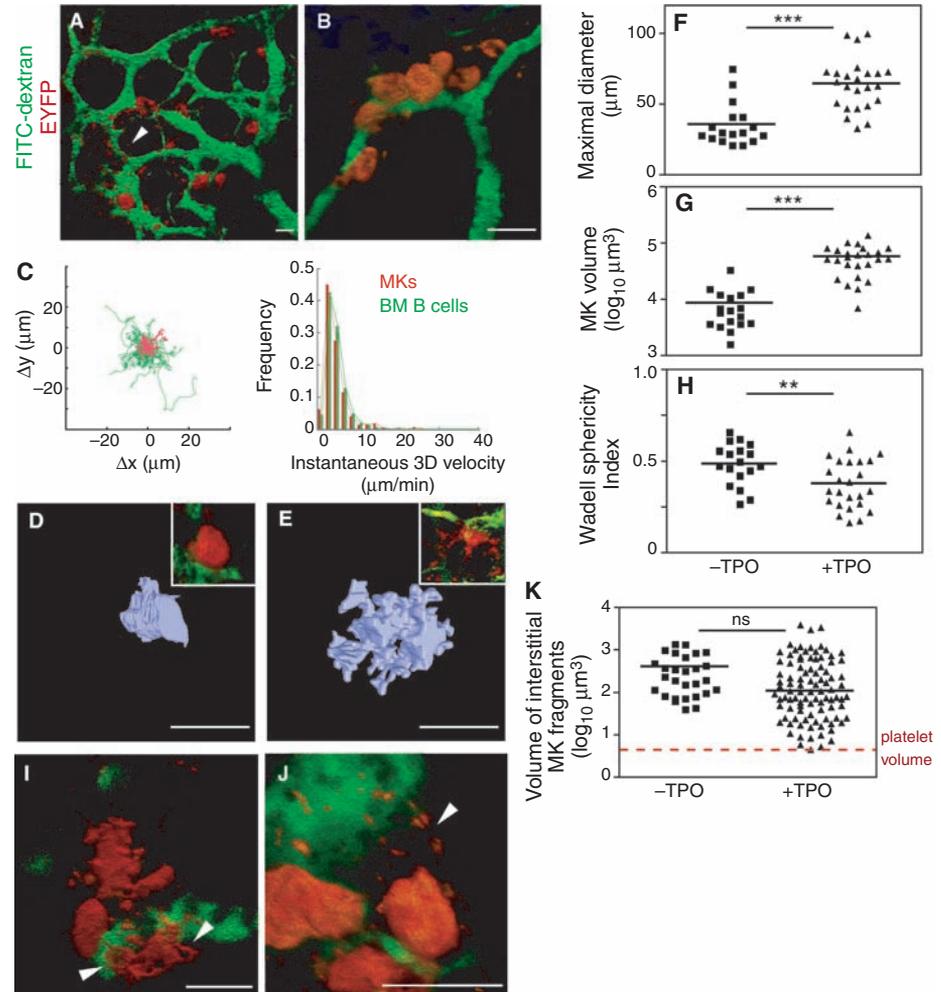

Fig. 1. Localization of EYFP⁺ MKs in BM of living mice. (**A**) EYFP⁺ MKs (red) and surrounding areas of fragmentation (arrowhead) in close proximity to BM sinusoids, which were outlined by intravenous injection of FITC-dextran (green). (**B**) Clusters of MKs along a BM sinusoidal vessel. (**C**) Cumulated tracks and instantaneous 3D velocities of BM MKs (red) and B lymphocytes (green). One representative of four movies for B cells, combined with cumulative data from four MK movies, is shown. (**D** and **E**) Representative 3D reconstructions of MKs from time-lapse MP-IVM; insets show renderings of intravital recordings. (**F** to **H**) Maximal diameters (F), volumes (G), and Wadell sphericity indices (H) of MKs in BM cavities of mice without (squares) or after (triangles) TPO treatment. **P < 0.01, ***P < 0.001; unpaired Student's t test. (**I**) Representative MKs with proplatelet-like protrusions (arrowheads). (**J**) Zones of aligned EYFP⁺ interstitial fragments close to an MK (arrowhead), possibly tethered to the cell body. Scale bars in (A), (B), (D), (E), (I), and (J), 50 μm. (**K**) Volumes of interstitial MK fragments with or without apparent connection to MK cell bodies and with or without TPO treatment. The dashed line denotes mean platelet volume. Data were compared with an unpaired Student's t test. ns, not significant. Horizontal bars in [(F) to (H)] and (K) indicate means.

tions, we determined MK volumes, surface areas, and Wadell sphericity indices (Fig. 2, F to H). Small MKs displayed a higher average sphericity index than large cells, indicating that the latter were less compact and shaped more

irregularly. These findings agree with morphological changes recorded in cultured MKs before proplatelet formation (3, 5) and hold true whether TPO was administered or not (fig. S4), confirming that TPO does not alter MK differentiation

qualitatively (23). Size and shape parameters of MKs that were actively shedding intravascular fragments were statistically similar to those of large nonshedding MKs (Fig. 2, F to H). Thus, vascular release of MK fragments occurred

Fig. 2. Intravascular MK fragmentation. (**A**) EYFP$^+$ MK (red) with proplatelet extensions inside BM sinusoids (see circles), which were demarcated by FITC-dextran injection (green). Numbers at top right in each panel denote image depth in μm. (**B**) Volume of EYFP$^+$ fragments released from MKs into BM sinusoids (bar represents mean: 3295 μm^3). (**C**) Apparent pseudopodium elaboration (arrowhead) by a perivascular MK. (**D**) Presence of a very large MK fragment in a sinusoidal vessel, with upstream accumulation (arrowhead) of FITC-dextran tracer. (**E**) Intravascular shedding of a MK fragment (arrowhead). Numbers at top left in each panel correspond to minutes and seconds. Scale bars in (A) and (C) to (E), 50 μm. (**F** to **H**) Volumes (F), surface areas (G), and Wadell sphericity indices (H) of small and large nonshedding MKs and of MKs captured in the process of shedding intravascular fragments. Data were analyzed with one-way analysis of variance tests with Bonferroni's post-test. *$P < 0.05$, **$P < 0.01$. Horizontal bars in (B) and (F) to (H) indicate means.
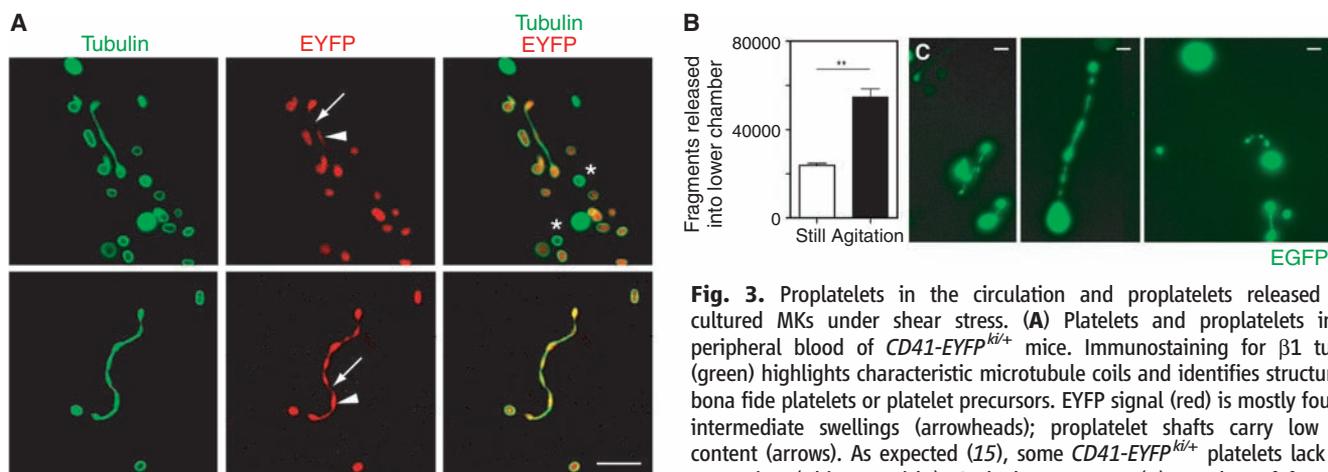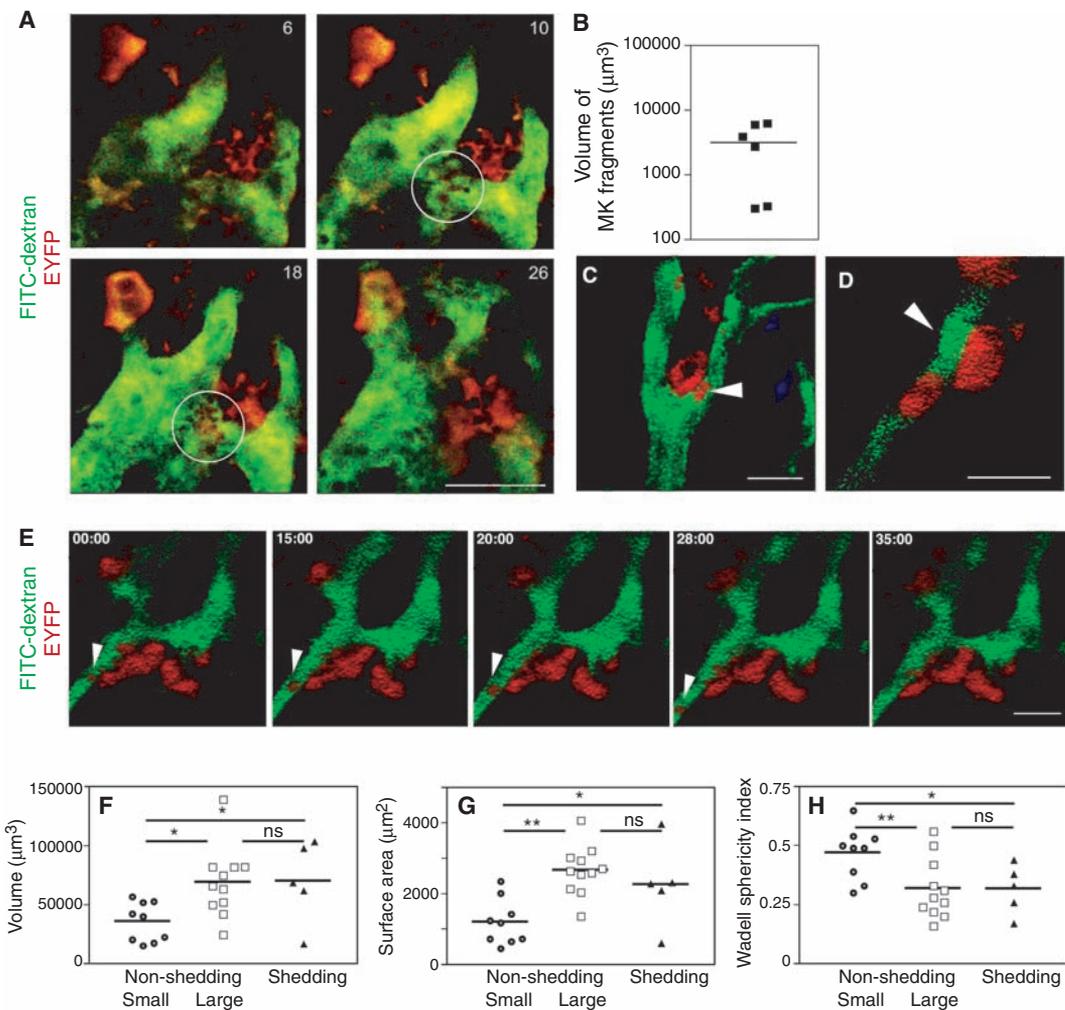

Fig. 3. Proplatelets in the circulation and proplatelets released from cultured MKs under shear stress. (**A**) Platelets and proplatelets in the peripheral blood of *CD41-EYFP$^{ki/+}$* mice. Immunostaining for β1 tubulin (green) highlights characteristic microtubule coils and identifies structures as bona fide platelets or platelet precursors. EYFP signal (red) is mostly found in intermediate swellings (arrowheads); proplatelet shafts carry low EYFP content (arrows). As expected (15), some *CD41-EYFP$^{ki/+}$* platelets lack EYFP expression (white asterisks). Scale bar, 10 μm. (**B**) Number of fragments released through 5-μm pores into lower transwell chambers, with (black bar) or without (white bar) agitation after mouse MKs were transduced with EGFP-expressing retrovirus and cultured to maturity. Means of triplicates are shown from one of two similar experiments; error bars indicate SEM. **$P < 0.01$; Student's *t* test. (**C**) Morphology of EGFP$^+$ MK fragments released through transwell filters after agitation. Scale bars, 10 μm.

concomitant to the expansion of MK size and loss of sphericity, most likely late in MK maturation, as predicted by proplatelet-based models of thrombopoiesis.

Because most shed MK fragments exceeded platelet dimensions, we inferred the presence of proplatelets in the systemic circulation, as proposed by Behnke (24). Indeed, beaded proplatelets and barbell-shaped platelet pairs (Fig. 3A) carrying characteristic β1-tubulin⁺ marginal bands (25) were readily identified in peripheral blood of *CD41-EYFP^{ki/+}* mice. Proplatelet morphogenesis is thought to continue in peripheral blood to engender individual platelets (24), possibly assisted by intravascular shear forces in pulmonary arterioles. This idea is consistent with observations that proplatelet counts are higher in prepulmonary vessels than in postpulmonary vessels (26), whereas platelet counts are higher in the latter (27).

Our observations raise the possibility that blood flow–induced shear stress [1.3 to 4.1 dynes/cm^2 in BM sinusoids (13)] may help separate intravascular cell fragments from the MK proper. Thus, we reasoned that mature MKs may be particularly susceptible to such forces in vitro. Indeed, MKs cultured on top of 5-μm transwells shed significantly more proplatelet-like fragments into the lower chamber when they were gently agitated as compared with MKs in static cultures (Fig. 3, B and C). Together with our MP-IVM observations, these results support the idea that intravascular release of fragments protruding from mature MKs is aided by hydrodynamic fluid shear in BM sinusoids.

Our in vivo observations permit refinement of thrombopoiesis models. Although cell growth and maturation, early events in MK ontogeny, are modulated by factors like TPO, later steps may be directed by chemokines or by localized expression of ligands for MK surface receptors. For example, CXCL12 (stromal-derived factor 1) is a potent MK chemoattractant (7), and fibrinogen present along BM sinusoids promotes proplatelet formation through $\alpha_{IIb}\beta_3$ integrin on MKs (28). However, newly synthesized platelets entering BM microvessels must avoid precocious activation and local clotting when they traverse the subendothelial space. We propose that MKs may circumvent this problem by extending voluminous processes into the lumen of local sinusoidal vessels. These processes are sheared off and may serve as an intravascular source of new platelets. Our observations also provide evidence for partial MK fragmentation within the BM interstitium, but further studies will be needed to determine if these structures give rise to viable platelets or serve other local functions.

References and Notes

1. R. P. Becker, P. P. De Bruyn, *Am. J. Anat.* **145**, 183 (1976).
2. J. M. Radley, G. Scurfield, *Blood* **56**, 996 (1980).
3. E. S. Choi, J. L. Nichol, M. M. Hokom, A. C. Hornkohl, P. Hunt, *Blood* **85**, 402 (1995).
4. E. M. Cramer et al., *Blood* **89**, 2336 (1997).
5. P. Lecine et al., *Blood* **92**, 1608 (1998).
6. A. Eldor et al., *Blood Cells* **17**, 447 (1991).
7. S. T. Avecilla et al., *Nat. Med.* **10**, 64 (2004).
8. J. E. Italiano Jr., P. Lecine, R. A. Shivdasani, J. H. Hartwig, *J. Cell Biol.* **147**, 1299 (1999).
9. M. A. Lichtman, J. K. Chamberlain, W. Simon, P. A. Santillo, *Am. J. Hematol.* **4**, 303 (1978).
10. E. Yamada, *Acta Anat.* **29**, 267 (1957).
11. D. Zucker-Franklin, S. Petursson, *J. Cell Biol.* **99**, 390 (1984).
12. G. Kosaki, *Int. J. Hematol.* **81**, 208 (2005).
13. I. B. Mazo et al., *J. Exp. Med.* **188**, 465 (1998).
14. Materials and Methods are available as supporting material on *Science* Online.
15. J. Zhang et al., *Exp. Hematol.* **35**, 490 (2007).
16. K. Kaushansky, *Blood* **86**, 419 (1995).
17. H. Schulze et al., *Blood* **107**, 3868 (2006).
18. S. R. Patel, J. H. Hartwig, J. E. Italiano Jr., *J. Clin. Invest.* **115**, 3348 (2005).
19. S. R. Patel et al., *Blood* **106**, 4076 (2005).
20. C. Poujol et al., *Blood* **92**, 2012 (1998).
21. M. Tavassoli, *Blood* **55**, 537 (1980).
22. K. Kabaya et al., *Stem Cells* **14**, 651 (1996).
23. S. Bunting et al., *Blood* **90**, 3423 (1997).
24. O. Behnke, A. Forer, *Eur. J. Haematol. Suppl.* **61**, 3 (1998).
25. P. Lecine, J. E. Italiano Jr., S. W. Kim, J. L. Villeval, R. A. Shivdasani, *Blood* **96**, 1366 (2000).
26. P. J. Handagama, B. F. Feldman, N. C. Jain, T. B. Farver, C. S. Kono, *Am. J. Vet. Res.* **48**, 962 (1987).
27. W. H. Howell, D. D. Donahue, *J. Exp. Med.* **65**, 177 (1937).
28. M. K. Larson, S. P. Watson, *Blood* **108**, 1509 (2006).
29. We thank A. Moseman, H. Leung, J. Richardson, and I. Mazo for advice. This work was funded by NIH grants HL56949 to U.H.v.A., HL63143 to R.A.S., and HL068130 to J.E.I. T.J. is a fellow of the Swiss National Science Foundation, T.Go. is a fellow, and S.M. is a Heisenberg fellow of the Deutsche Forschungsgemeinschaft. The authors do not have competing financial interests.